molbank

MDPI

Communication

Supramolecular Self-Assembly of the Zwitterionic Sn(IV)-Porphyrin Complex

Nirmal Kumar Shee and Hee-Joon Kim *

Department of Chemistry and Bioscience, Kumoh National Institute of Technology, Gumi 39177, Republic of Korea; nirmalshee@gmail.com
* Correspondence: hjk@kumoh.ac.kr; Tel.: +82-54-4787822

Abstract: $[Sn(OSO_3)_2(TPy^HP)](HSO_4)_2{\cdot}8H_2O$ (**1**), an ionic Sn(IV)-porphyrin complex, was prepared by reacting $[Sn(OH_2)_2TPyP]$ with dilute sulfuric acid. X-ray structural analysis revealed that the zwitterionic $[Sn(OSO_3)_2TPy^HP]^{2+}$ species consists of two anionic axial Sn–O–SO_3 units and four peripheral pyridinium moieties, with an overall dicationic charge balanced by two hydrogen sulfate (HSO_4^-) counter-anions. Ionic hydrogen bonding between the oxygen atoms of axial sulfato ligands and the peripheral pyridinium groups of adjacent Sn(IV)-porphyrin cations led to the formation of a 1D channel filled with counter-anions and water molecules. The supramolecular self-assembly of **1** was further characterized using various spectroscopic techniques, including ^{1}H NMR spectroscopy, elemental analysis, ESI-mass spectrometry, UV-vis spectroscopy, fluorescence spectroscopy, FT-IR spectroscopy, thermogravimetric analysis (TGA), and powder X-ray diffractometry. The zwitterionic $[Sn(OSO_3)_2TPy^HP]^{2+}$ complex is a structurally well-defined complementary scaffold involved in supramolecular self-assembly. This novel class of ion-assembled metalloporphyrin is a potential functional porphyrin material used in ion exchange applications.

Keywords: Sn(IV)-porphyrin; zwitterion; self-assembly; supramolecule; ionic hydrogen bonding

check for updates

Citation: Shee, N.K.; Kim, H.-J. Supramolecular Self-Assembly of the Zwitterionic Sn(IV)-Porphyrin Complex. *Molbank* **2023**, *2023*, M1723. https://doi.org/10.3390/M1723

Academic Editor: R. Alan Aitken

Received: 22 August 2023
Revised: 7 September 2023
Accepted: 11 September 2023
Published: 12 September 2023

Copyright: © 2023 by the authors. Licensee MDPI, Basel, Switzerland. This article is an open access article distributed under the terms and conditions of the Creative Commons Attribution (CC BY) license (https://creativecommons.org/licenses/by/4.0/).

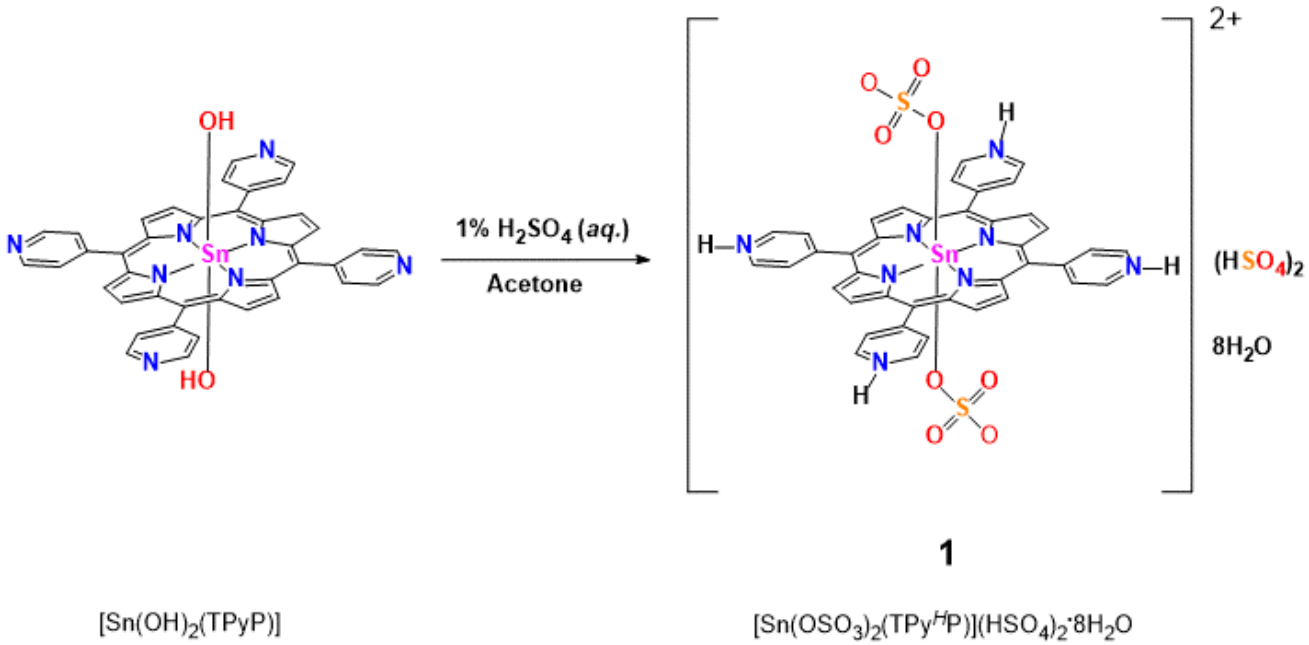
1. Introduction

The supramolecular assembly of metalloporphyrins with unique structures and functions provides important insights into developing photoelectronically active materials [1–9]. Noncovalent intermolecular interactions, such as hydrogen bonding [10,11], π-π stacking [12–14], and metal–ligand coordination [15–18], have mainly been used for the supramolecular assembly of metalloporphyrins. In contrast, ionic assembly is usually achieved via the association of separate ionic species with opposite charges [19]. We studied the ionic assemblies of charged Sn(IV)-porphyrin complexes in order to develop photofunctional porphyrin nanomaterials. Octahedral Sn(IV)-porphyrin geometry is a very attractive skeleton that can be used for constructing self-assembled metalloporphyrin arrays, as cooperative interactions between axial ligands and peripheral functional groups in such complexes create interesting supramolecular arrays [20–26]. Herein, we report the supramolecular self-assembly of zwitterionic Sn(IV)-porphyrin complexes. X-ray crystallographic analysis revealed that intermolecular hydrogen bonding between cationic pyridinium groups and axially coordinated sulfato ligands is responsible for the self-assembly of the zwitterionic Sn(IV)–porphyrin complex.

2. Results and Discussion

The axial hydroxo ligands of Sn(IV)-porphyrins were easily acidolyzed by oxyacids to adopt new oxyanion ligands [27,28]. $Sn(OH)_2TPyP$ reacted with H_2SO_4 in a water–acetone mixture to form $[Sn(OSO_3)_2(TPy^HP)](HSO_4)_2{\cdot}8H_2O$ (**1**) (Scheme 1); the details of this reaction are provided in the Experimental section. Complex **1** was fully characterized using various spectroscopic techniques, including X-ray crystallographic analysis, ^{1}H

NMR spectroscopy, elemental analysis, ESI-MS, solid-state and solution-phase UV-vis spectroscopy, fluorescence spectroscopy, FT-IR spectroscopy, thermogravimetric analysis (TGA), and powder X-ray diffractometry (XRD).



Scheme 1. Preparation of **1**.

2.1. X-ray Crystal Structure Analysis

A block-shaped violet single crystal of **1** suitable for X-ray crystallography was readily obtained via the slow diffusion of acetone into a 1% acidic solution (H_2SO_4) of $Sn(OH)_2$TPyP; **1** was crystalized in a monoclinic system in the *I* 2/*a* centrosymmetric space group. Detailed crystallographic data and structural refinement parameters are provided in Table S1, with selected bond lengths and angles listed in Table S2.

The molecular structure of the zwitterionic Sn(IV)-porphyrin unit in **1** revealed that the Sn(IV) atom is octahedrally coordinated (Figure 1). The equatorial plane was formed by four N atoms of the porphyrin ring, whereas the axial positions were occupied by the O atoms of the two sulfato ligands. The axial sulfato ligand bonded to the Sn(IV)-porphyrin center was symmetrically equivalent. In a previous report, the reaction of $Sn(OH)_2$TPyP with a 1% nitric acid solution led to the formation of a hexa-cationic $[Sn(OH_2)_2TPy^HP]^{6+}$ species [23] balanced by six NO_3^- anions. In this case, the axial hydroxyl and pyridine groups were protonated to form a hexa-cationic $[Sn(OH_2)_2TPy^HP]^{6+}$ species stabilized by six nitrate counter-anions. Unlike HNO_3, treatment with H_2SO_4 was shown to form axial Sn–O–SO_3 bonds in **1**. Consequently, two anionic axial Sn–O–SO_3 and four cationic pyridinium peripheral moieties formed a zwitterionic $[Sn(OSO_3)_2TPy^HP]^{2+}$ species. The overall dicationic charge was balanced by two hydrogen sulfate (HSO_4^-) counter-anions.

The two equivalent Sn–N bonds were determined to have lengths of 2.079(2) and 2.082(2) Å. The average bond length was slightly shorter than that observed for the $[Sn(OH_2)_2TPy^HP]^{6+}$ species (2.083 Å). The axial Sn–O bond was determined to have a length of 2.103(2) Å, which is similar to that observed for $[Sn(TPP)(CH_3SO_3)_2]$ (2.1184(18) Å) [29]. The O–S bond (1.5362(16) Å) in the Sn–O–SO_3 moiety was differentially longer than the other O–S bonds (1.4575(17), 1.4572(16), and 1.4698(17) Å) in the sulfato ligand, and significantly longer than that (1.5077 (19) Å) in $[Sn(TPP)(CH_3SO_3)_2]$.

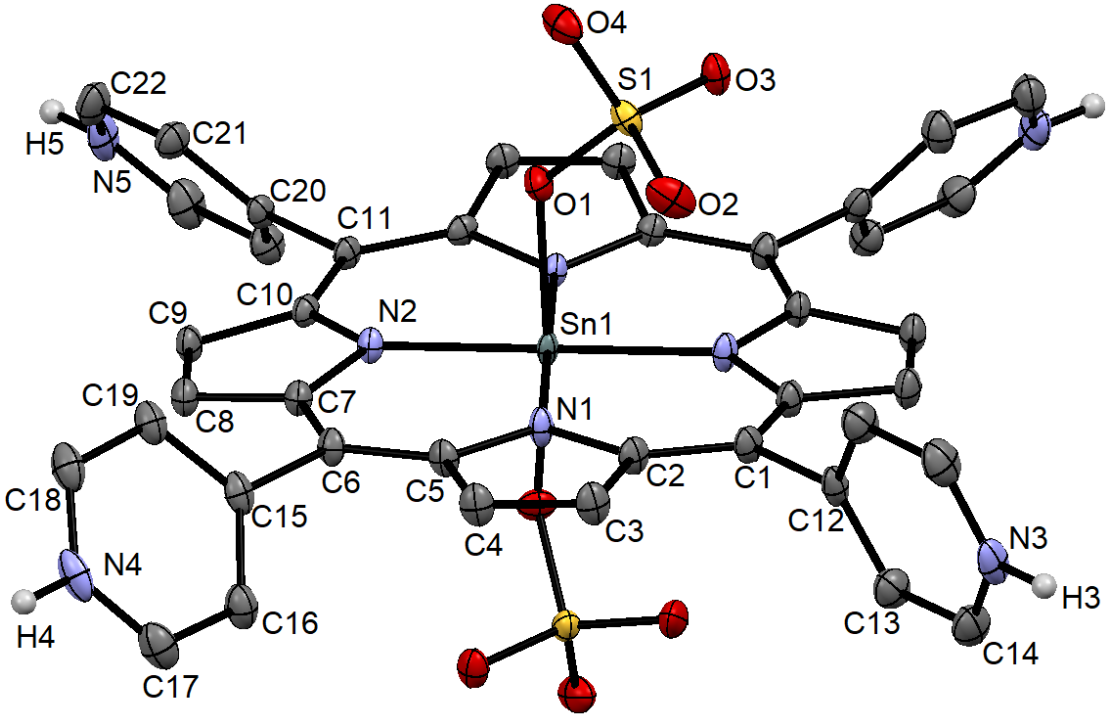


Figure 1. ORTEP diagram of the zwitterionic Sn(IV)–porphyrin complex formulated as $[Sn(OSO_3)_2TPy^HP]^{2+}$ in **1** drawn at a 50% probability level. All hydrogen atoms, except those on the pyridinium moieties, were omitted for clarity purposes. Color code: red, O; blue, N; cyan, Sn; gray, C; yellow, S; white, H.

The zwitterionic nature of $[Sn(OSO_3)_2TPy^HP]^{2+}$ was found to be a key factor in the supramolecular assembly of **1**. As shown in Figure 2, the anionic sulfato ligand acted as a hydrogen-bonded acceptor and interacted with the cationic pyridinium group (hydrogen-bonded donor) of the adjacent porphyrin moiety. The distances from the axial oxygen atom of the sulfato ligand to the hydrogen-bonded pyridinium nitrogen (O4···H4–N4) in the adjacent Sn(IV)-porphyrin complex were estimated to be 1.820 Å (O4···H4) and 2.698 Å (O4···N4), with the O4···H4–N4 angle determined to be 175.05°. Ionic hydrogen bonding between the anionic axial sulfato ligand and cationic pyridinium peripheral groups of the adjacent Sn(IV)-porphyrin complex led to a networked structure during the self-assembly of zwitterionic $[Sn(OSO_3)_2TPy^HP]^{2+}$. The overall dicationic charge of the Sn(IV)-porphyrin complex was balanced by two hydrogen sulfate (HSO_4^-) counter-anions.

As shown in Figure 3, **1** exhibited a 1D network packing structure. More importantly, the overall combination of the 1D network structures of **1** led to an open network with 1D channels of uniform pore size (10 × 8 Å). The channels were occupied by counter-anions and water molecules (Figure 4), and this channeled porous structure was expected to facilitate anion exchange.

2.2. Spectroscopic Characterization

The ^{1}H NMR spectrum of **1** in D_2O (Figure S1) revealed that the β-pyrrolic protons resonate as a singlet at 9.58 ppm. On the other hand, the pyridine protons appeared as a doublet at 9.40 ppm (for the 2,6 positions) and 9.12 ppm (for the 3,5 positions). The molecular formula of the $[Sn(OSO_3)_2TPy^HP]^{2+}$ unit and its dication characteristics were confirmed by ESI-mass spectrometry (Figure S2). The peak with m/z 466.05 was assigned to $[Sn(OSO_3)_2TPy^HP]^{2+}$(theoretically required 466.025), while that with m/z 129.36 was assigned to $[Sn(OH_2)_2TPy^HP]^{6+}$ (theoretically required 129.24). We also obtained satisfactory elemental analysis data (C, H, N, and S) for **1** following evacuation.

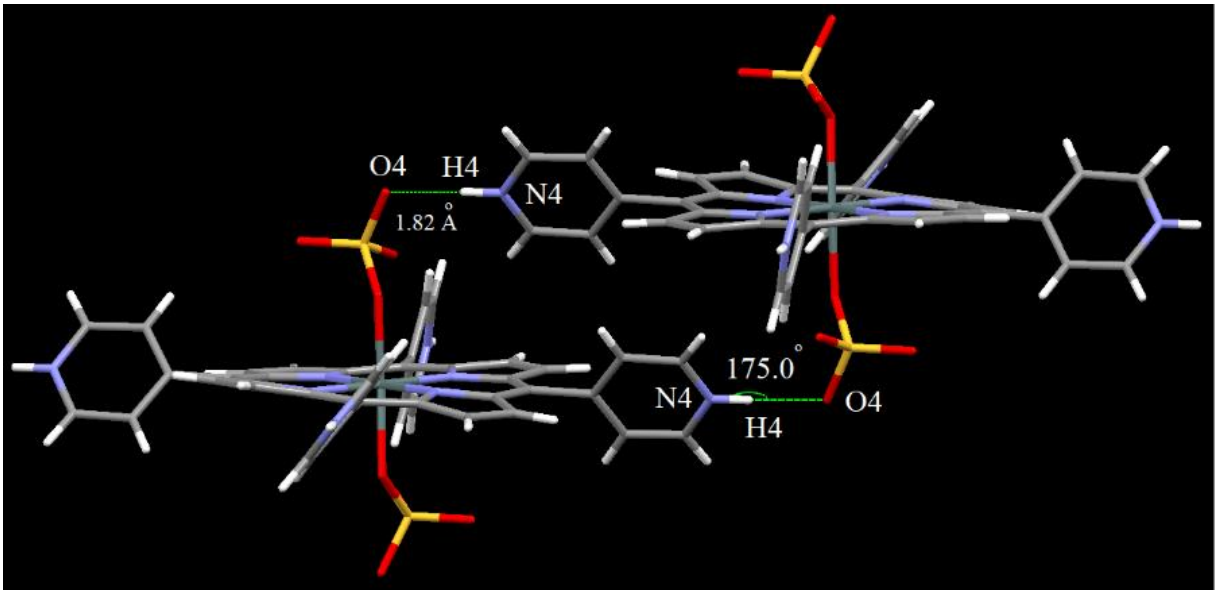


Figure 2. Ionic hydrogen bonds between the anionic axial sulfato ligand and cationic pyridinium substituent in zwitterionic $[Sn(OSO_3)_2TPy^HP]^{2+}$ viewed along the *b*-axis.

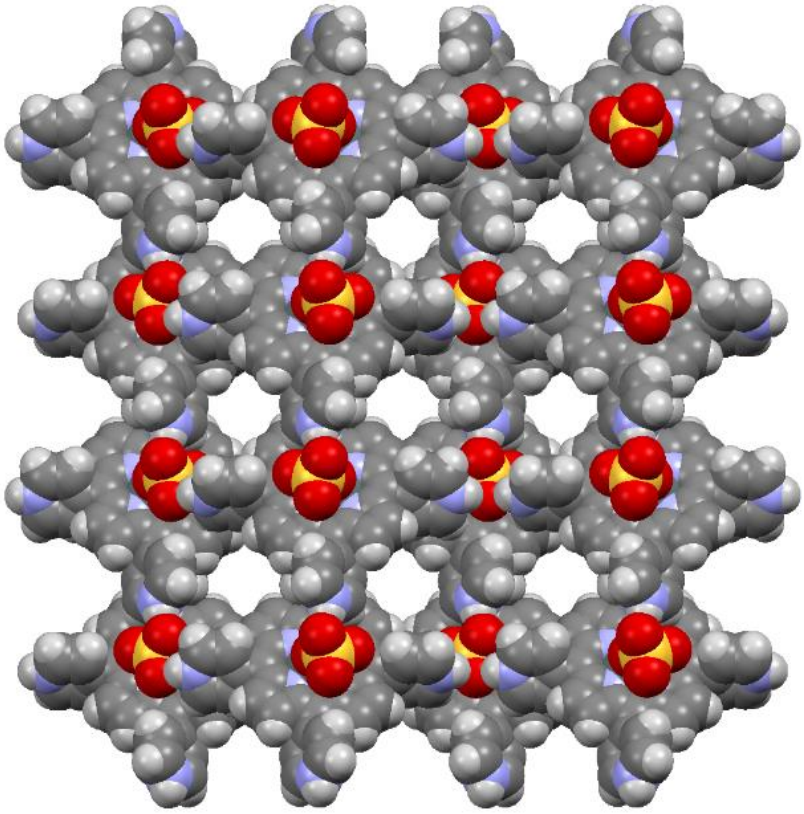


Figure 3. Packing diagram for **zwitterionic** Sn(IV)-porphyrin **complexes in 1** showing its regular arrays and 1D channels with space-filling representations along the crystallographic *a*-axis. Lattice solvent molecules and counter-anions were omitted for clarity purposes.

The optical properties of **1** were examined both in the solid and solution phases. The UV-visible absorption spectrum of the aqueous solution showed a sharp Soret absorption band at 415 nm, with Q bands at 514, 552, and 588 nm (Figure S3a). This absorption characteristic was almost identical to that of $[Sn(OH)_2(TPyP)]$, which appeared at 415, 514, 553, and 589 nm. This meant that the stability of the Sn-O bond for the two complexes was

not different in solution. On the other hand, the solid-state spectrum showed very broad absorption bands with a strong Soret absorption band at around 430 nm and Q-bands in the 540–690 nm range (Figure S3b). The fluorescence spectra of **1** are shown in Figure S4; while **1** shows emission bands at 600 and 647 nm in aqueous solution, a single emission band was observed at 645 nm in the solid state (Figure S4).

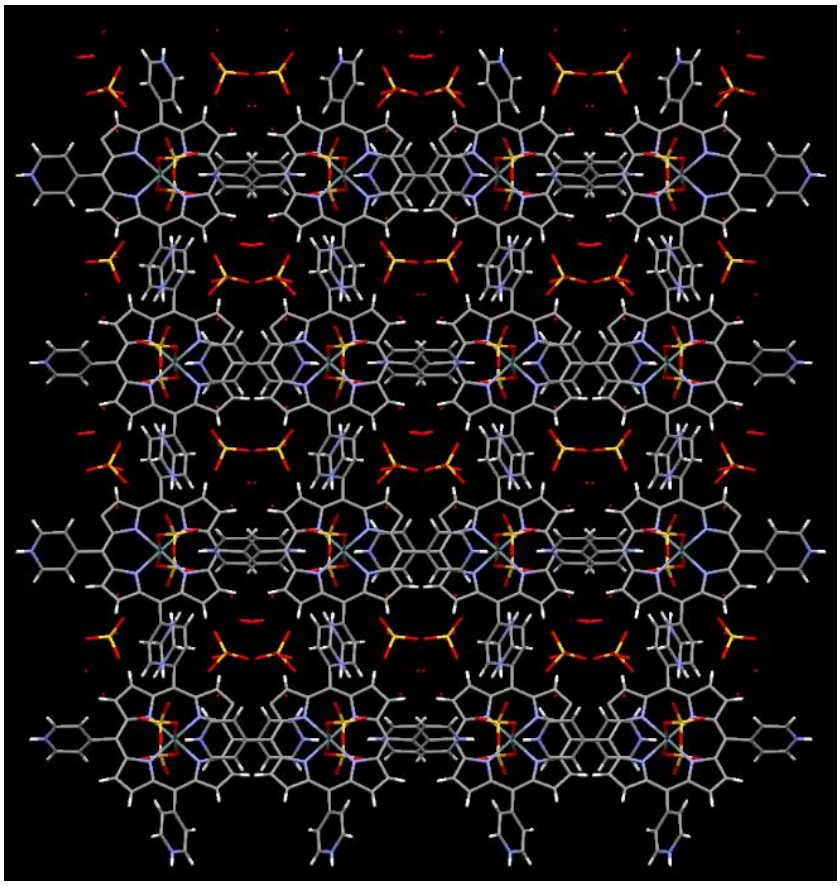


Figure 4. Crystal packing for **1** viewed along the crystallographic *a*-axis, which revealed that counter-anions and lattice solvent molecules were included in the 1D channels.

The Fourier transform infrared (FT-IR) spectrum of **1** is shown in Figure S5. The absence of a characteristic O-H stretching peak for Sn-OH (~3600 cm^{-1}) was consistent with the X-ray crystal structure of **1**. Characteristic S-O stretching and bending peaks were observed at 1150 and 575 cm^{-1}, which confirmed the presence of hydrogen sulfate anions. The thermal stability of crystalline **1** was examined by thermogravimetric analysis (TGA) (Figure S6); **1** lost approximately 10 wt% of its weight when heated to 100 °C, which was likely due to the removal of clathrate water molecules. The framework of **1** seemed to be thermally stable to ~350 °C, since substantial weight was only lost above ~400 °C. The powder XRD patterns of **1** shown in Figure S7 indicated that the crystallinity and framework were virtually maintained even after drying treatment. The slight discrepancy compared to the simulated pattern was probably due to the loss of solvent molecules.

3. Materials and Methods

Commercially available chemicals were used without further purification. *Trans*-dihydroxo[5,10,15,20-tetrakis(4-pyridyl)porphyrinato]Sn(IV) ([$Sn(OH)_2$(TPyP)]) was prepared using a previously reported procedure [21]. Elemental analysis was performed using a ThermoQuest EA 1110 analyzer (Thermo Fisher Scientific, Waltham, MA, USA). ^{1}H NMR spectra were obtained using a Bruker BIOSPIN/AVANCE III 400 spectrometer at 293 K (Bruker BioSpin GmbH, Silberstreifen, Rheinstetten, Germany). Electrospray ionization

(ESI) mass spectra were recorded using a Thermo Finnigan linear ion trap quadrupole mass spectrometer (Thermo Fisher Scientific, Waltham, MA, USA). UV-Vis absorption spectra were obtained using a Shimadzu UV-3600 spectrophotometer (Shimadzu, Tokyo, Japan). Fluorescence spectra were acquired using a Shimadzu RF-5301PC fluorescence spectrophotometer (Shimadzu, Tokyo, Japan). FT-IR spectra were obtained using a Shimadzu FTIR-8400S spectrophotometer (Shimadzu, Tokyo, Japan). Thermogravimetric analysis (TGA) was performed using an Auto-TGA Q500 instrument (TA Instruments, New Castle, DE, USA). Powder X-ray diffractometry (XRD) was performed using a Bruker AXS D8 Advance powder X-ray diffractometer (Bruker, Billerica, MA, USA).

*3.1. Synthesis of [Sn(OSO$_3$)$_2$(TPy^{H}P)](HSO$_4$)$_2$·8H$_2$O (**1**)*

[Sn(OH)$_2$(TPyP)] (154.0 mg, 0.20 mmol) was dissolved in 1% aqueous sulfuric acid (3 mL), and acetone (30 mL) was layered over for slow diffusion at room temperature. The solution was allowed to stand for 7 d in the dark, which produced block-shaped violet crystals of **1** suitable for X-ray crystallography. The dark-violet crystalline compound was collected by filtration, washed twice with acetone, and air-dried. Yield: 210 mg (83%). ^{1}H NMR (400 MHz, D$_2$O): δ 9.58 (s, 8H, H-pyrrole), 9.40 (d, J = 6.5 Hz, 8H, H$_{2,6}$-pyridine), and 9.12 (d, J = 6.3 Hz, 8H, and H$_{3,5}$-pyridine). FT-IR (KBr pellet, ν/cm^{-1}): 3110 (w), 3070 (w), 2780 (br), 2580(br), 1630 (vs), 1500 (s), 1230 (s), 1150 (w), 1100 (w), 1030 (vs), 995 (w), 840 (s), 790 (s), 725 (w), 650 (w), and 570 (vs). UV–vis (H$_2$O, nm): λ_{max} (log ε) 415 (4.73), 514 (3.04), 552 (3.68), and 588 (2.98). UV–vis (solid, nm): λ_{max} 430, 522, 570, and 609. Emission (water, nm): λ_{nm} 600 and 647. Emission (solid, nm): λ_{nm} 645 (br). Elemental analysis of the evacuated sample: anal. calcd. for C$_{40}$H$_{30}$N$_8$O$_{16}$S$_4$Sn (%): C, 42.68; H, 2.69; N, 9.95; S, 11.39; and R, 33.29. Found: C, 42.37; H, 2.86; N, 9.77; S, 12.27; and R, 32.73. ESI-mass: m/z 466.05 for [Sn(OSO$_3$)$_2$TPy^{H}P]$^{2+}$ (required: 466.025) and m/z 129.36 for [Sn(OH$_2$)$_2$TPy^{H}P]$^{6+}$ (required: 129.24).

3.2. X-ray Crystal Structure Determination

A single crystal of **1** suitable for X-ray analysis was collected using Paraton-*N* hydrocarbon oil on a glass fiber and mounted on a Bruker APEX-II CCD diffractometer equipped with a graphite monochromated Mo Kα (l = 0.71073 Å) radiation source and a CCD detector. The data were collected at 130 K under a cold flowing N$_2$. The structure was solved using direct methods and refined with the full-matrix least-squares method using the SHELXTL package [30,31] and graphical works using the Olex2 software package (version 1.5) [32]. Crystallographic and additional data collection and refinement details are summarized in Table S1. Non-hydrogen atoms were refined using anisotropic thermal parameters. The hydrogen atoms bonded to carbon and nitrogen were included at their geometric positions and given thermal parameters equivalent to 1.2 times those of the atoms to which they were attached. The hydrogen sulfate counter-anions and clathrate water molecules were refined without hydrogen atoms owing to their positional disorder. The final full-matrix least-squares refinement of F^2 converged to R_1 = 0.0335 (all data) and wR_2 = 0.0835 ($I > 2\sigma(I)$), with a GOF = 1.061.

4. Conclusions

We studied supramolecular self-assembly based on a zwitterionic Sn(IV)porphyrin obtained by reacting [Sn(OH$_2$)$_2$TPyP] with sulfuric acid. X-ray crystallography revealed that the zwitterionic [Sn(OSO$_3$)$_2$TPy^{H}P]$^{2+}$ complex consists of two anionic axial Sn–O–SO$_3$ units and four peripheral pyridinium moieties. The overall dicationic charge was balanced by two hydrogen sulfate (HSO$_4^-$) counter-anions. Ionic hydrogen bonding between the oxygen atom of the axial sulfato ligand and the pyridinium peripheral groups of the adjacent Sn(IV)–porphyrin complex led to the formation of a 1D channel filled with counter-anions and water molecules. The supramolecular self-assembly was fully characterized using various spectroscopic techniques, including ^{1}H NMR spectroscopy, elemental analysis, ESI-mass spectrometry, UV-vis spectroscopy, fluorescence spectroscopy, FT-IR spectroscopy,

thermogravimetric analysis, and powder XRD. The zwitterionic $[Sn(OSO_3)_2TPy^HP]^{2+}$ complex is a structurally well-defined complementary scaffold involved in supramolecular self-assembly. Our findings provide new opportunities for the development of functional porphyrin materials used in ion exchange applications.

Supplementary Materials: Table S1: Crystallographic data and structure refinement for **1**; Table S2: Selected bond lengths and angles in **1**; Figure S1: ^{1}H NMR spectrum of **1**; Figure S2: ESI-mass spectrum of **1**; Figure S3: UV-Vis spectra of **1**; Figure S4: Fluorescence spectra of **1**; Figure S5: FT-IR spectrum of **1**; Figure S6: TGA thermogram of **1**; Figure S7: Powder XRD pattern of **1**.

Author Contributions: Data curation, formal analysis, investigation, methodology, software, visualization, and writing—original draft preparation: N.K.S. Conceptualization, funding acquisition, project administration, resources, validation, writing—review, and editing: H.-J.K. All authors have read and agreed to the published version of the manuscript.

Funding: This work was supported by the National Research Foundation of Korea (NRF) (grant no. 2022R1F1A1074420), funded by the Korean government (MSIT).

Data Availability Statement: CCDC 2289182 contains supplementary crystallographic data for this paper. These data can be obtained free of charge via http://www.ccdc.cam.ac.uk/conts/retrieving.html (or from the CCDC, 12 Union Road, Cambridge, CB2 1EZ, UK; fax: +44-1223-336033; e-mail: deposit@ccdc.cam.ac.uk).

Acknowledgments: We thank Jaheon Kim and Hwa Jin Jo for their crystallographic analysis advice and initial synthetic work, respectively.

Conflicts of Interest: The authors declare no conflict of interest.

References

1. Chambron, J.-C.; Heitz, V.; Sauvage, J.-P. *The Porphyrin Handbook*; Kadish, K.M., Smith, K.M., Guilard, R., Eds.; Academic Press: San Diego, CA, USA, 2000; Volume 6, pp. 1–42.
2. Chou, J.-H.; Nalwa, H.S.; Kosal, M.E.; Rakow, N.A.; Suslick, K.S. Applications of Porphyrins and Metalloporphyrins to Materials Chemistry. In *The Porphyrin Handbook*; Kadish, K.M., Smith, K.M., Guilard, R., Eds.; Academic Press: San Diego, CA, USA, 2000; Volume 6, pp. 43–131.
3. Suslick, K.S.; Rakow, N.A.; Kosal, M.E.; Chou, J.-H. The materials chemistry of porphyrins and metalloporphyrins. *J. Porphyr. Phthalocyanines* **2000**, *4*, 407–413. [CrossRef]
4. Milic, T.N.; Chi, N.; Yablon, D.G.; Flynn, G.W.; Batteas, J.D.; Drain, C.M. Controlled hierarchical self-assembly and deposition of nanoscale photonic materials. *Angew. Chem. Int. Ed.* **2002**, *41*, 2117–2119. [CrossRef]
5. Drain, C.M.; Hupp, J.T.; Suslick, K.S.; Wasielewski, M.R.; Chen, X. A perspective on four new porphyrin-based functional materials and devices. *J. Porphyr. Phthalocyanines* **2002**, *6*, 243–258. [CrossRef]
6. Vinodu, M.; Goldberg, I. New assembly modes of porphyrin-based networks. *CrystEngComm* **2003**, *5*, 204–207. [CrossRef]
7. Goldberg, I. Crystal engineering of porphyrin framework solids. *Chem. Commun.* **2005**, *10*, 1243–1254. [CrossRef]
8. George, S.; Goldberg, I. Self-Assembly of Supramolecular Porphyrin Arrays by Hydrogen Bonding: New Structures and Reflections. *Cryst. Growth Des.* **2006**, *6*, 755–762. [CrossRef]
9. Hasobe, T. Photo-and electro-functional self-assembled architectures of porphyrins. *Phys. Chem. Chem. Phys.* **2012**, *14*, 15975–15987. [CrossRef]
10. Madueno, R.; Raisanen, M.T.; Silien, C.; Buck, M. Functionalizing hydrogen-bonded surface networks with self-assembled monolayers. *Nature* **2008**, *454*, 618–621. [CrossRef]
11. Ohkawa, H.; Takayama, A.; Nakajima, S.; Nishide, H. Cyclic Tetramer of a Metalloporphyrin Based on a Quadruple Hydrogen Bond. *Org. Lett.* **2006**, *8*, 2225–2228. [CrossRef]
12. Hunter, C.A.; Sanders, J.K.M. The nature of .Pi.-.Pi. Interactions. *J. Am. Chem. Soc.* **1990**, *112*, 5525–5534. [CrossRef]
13. Watson, M.D.; Fechtenkotter, A.; Müllen, K. Big Is Beautiful-"Aromaticity" Revisited from the Viewpoint of Macromolecular and Supramolecular Benzene Chemistry. *Chem. Rev.* **2001**, *101*, 1267–1300. [CrossRef]
14. Zang, L.; Che, Y.; Moore, J.S. One-Dimensional Self-Assembly of Planar π-Conjugated Molecules: Adaptable Building Blocks for Organic Nanodevices. *Acc. Chem. Res.* **2008**, *41*, 1596–1608. [CrossRef]
15. Northrop, B.H.; Zheng, Y.-R.; Chi, K.-W.; Stang, P.J. Self-Organization in Coordination-Driven Self-Assembly. *Acc. Chem. Res.* **2009**, *42*, 1554–1563. [CrossRef] [PubMed]
16. Horike, S.; Shimomura, S.; Kitagawa, S. Soft porous crystals. *Nat. Chem.* **2009**, *1*, 695–704. [CrossRef]
17. Farha, O.K.; Shultz, A.M.; Sarjeant, A.A.; Nguyen, S.T.; Hupp, J.T. Active-Site-Accessible, Porphyrinic Metal-Organic Framework Materials. *J. Am. Chem. Soc.* **2011**, *133*, 5652–5655. [CrossRef]

18. Lee, C.Y.; Farha, O.K.; Hong, B.J.; Sarjeant, A.A.; Nguyen, S.T.; Hupp, J.T. Light-Harvesting Metal-Organic Frameworks (MOFs): Efficient Strut-to-Strut Energy Transfer in Bodipy and Porphyrin-Based MOFs. *J. Am. Chem. Soc.* **2011**, *133*, 15858–15861. [CrossRef] [PubMed]
19. Faul, C.F.J.; Antonietti, M. Ionic self-assembly: Facile synthesis of supramolecular materials. *Adv. Mater.* **2003**, *15*, 673–683. [CrossRef]
20. Fallon, G.D.; Langford, S.J.; Lee, M.A.-P.; Lygris, E. Self-assembling Mixed Porphyrin Trimers—The Use of Diaxial Sn(IV) Porphyrin Phenolates as an Organising Precept. *Inorg. Chem. Commun.* **2002**, *5*, 715–718. [CrossRef]
21. Jo, H.J.; Jung, S.H.; Kim, H.-J. Synthesis and Hydrogen-Bonded Supramolecular Assembly of *trans*-Dihydroxotin(IV) Tetrapyridylporphyrin Complexes. *Bull. Korean Chem. Soc.* **2004**, *25*, 1869–1873.
22. Dvivedi, A.; Pareek, Y.; Ravikanth, M. Sn^{IV} Porphyrin Scaffolds for Axially Bonded Multiporphyrin Arrays: Synthesis and Structure Elucidation by NMR Studies. *Chem. Eur. J.* **2014**, *20*, 4481–4490. [CrossRef]
23. Jo, H.J.; Kim, S.H.; Kim, H.-J. Supramolecular Assembly of Tin(IV) Porphyrin Cations Stabilized by Ionic Hydrogen-Bonding Interactions. *Bull. Korean Chem. Soc.* **2015**, *36*, 2348–2351. [CrossRef]
24. Amati, A.; Cavigli, P.; Demitri, N.; Natali, M.; Indelli, M.T.; Iengo, E. Sn(IV) Multiporphyrin Arrays as Tunable Photoactive Systems. *Inorg. Chem.* **2019**, *58*, 4399–4411. [CrossRef] [PubMed]
25. Shee, N.K.; Lee, C.-J.; Kim, H.-J. Hexacoordinated Sn(IV) porphyrin-based square-grid frameworks exhibiting selective uptake of CO_2 over N_2. *Bull. Korean Chem. Soc.* **2022**, *43*, 103–109. [CrossRef]
26. Kim, H.-J. Assembly of Sn(IV)-Porphyrin Cation Exhibiting Supramolecular Interactions of Anion···Anion and Anion···π Systems. *Molbank* **2022**, *2022*, M1454. [CrossRef]
27. Hawley, J.C.; Bampos, N.; Abraham, R.J.; Sanders, J.K.M. Carboxylate and carboxylic acid recognition by tin (IV) porphyrins. *Chem. Commun.* **1998**, *6*, 661–662. [CrossRef]
28. Chen, Q.-C.; Xiao, Z.-Y.; Fite, S.; Mizrahi, A.; Fridman, N.; Zhan, X.; Keisar, O.; Cohen, Y.; Gross, Z. Tuning Chemical and Physical Properties of Phosphorus Corroles for Advanced Applications. *Chem. Eur. J.* **2019**, *25*, 11383–11388. [CrossRef]
29. Singh, A.P.; Kim, H.-J. Bis(methanesulfonato-κ O)(5,10,15,20-tetraphenylporphyrinato-κ^4*N*,*N*′,*N*″,*N*‴)tin(IV) chloroform trisolvate. *Acta Cryst.* **2012**, *E68*, m626. [CrossRef]
30. Sheldrick, G.M. A short history of SHELX. *Acta Crystallogr. Sect. A Found. Crystallogr.* **2008**, *64*, 112–122. [CrossRef]
31. Bruker. *SHELXTL (Ver. 6.10): Program for Solution and Refinement of Crystal Structures*; Bruker AXS Inc.: Madison, WI, USA, 2000.
32. Dolomanov, O.V.; Bourhis, L.J.; Gildea, R.J.; Howard, J.A.K.; Puschmann, H. OLEX2: A Complete Structure Solution, Refinement and Analysis Program. *J. Appl. Crystallogr.* **2009**, *42*, 339–341. [CrossRef]

Disclaimer/Publisher's Note: The statements, opinions and data contained in all publications are solely those of the individual author(s) and contributor(s) and not of MDPI and/or the editor(s). MDPI and/or the editor(s) disclaim responsibility for any injury to people or property resulting from any ideas, methods, instructions or products referred to in the content.